Novel Quaternary Ammonium-Based Cationic Surfactants: Synthesis, Surface Activity and Evaluation as Corrosion Inhibitors for C1018 Carbon Steel in Acidic Chloride Solution

Hany M. Abd El-Lateef, Ahmed H. Tantawy & Antar A. Abdelhamid

Journal of Surfactants and Detergents

ISSN 1097-3958
Volume 20
Number 3

J Surfact Deterg (2017) 20:735-753
DOI 10.1007/s11743-017-1947-7

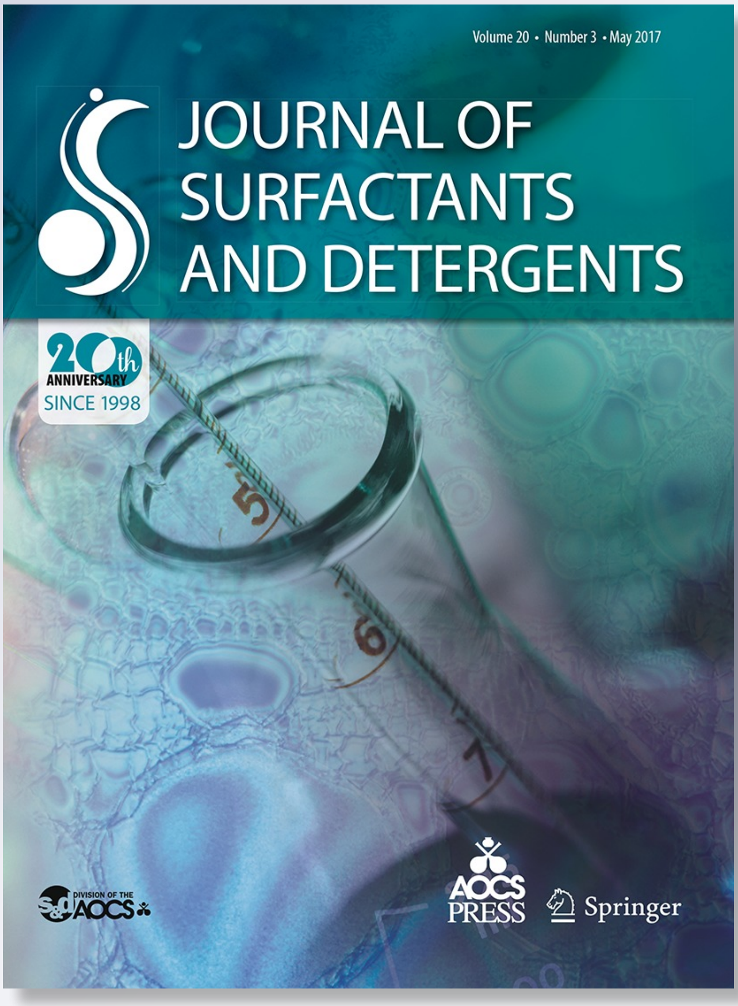

J Surfact Deterg (2017) 20:735–753
DOI 10.1007/s11743-017-1947-7

ORIGINAL ARTICLE

Novel Quaternary Ammonium-Based Cationic Surfactants: Synthesis, Surface Activity and Evaluation as Corrosion Inhibitors for C1018 Carbon Steel in Acidic Chloride Solution

Hany M. Abd El-Lateef[1] · **Ahmed H. Tantawy**[2] · **Antar A. Abdelhamid**[1]

Received: 13 October 2015 / Accepted: 6 March 2017 / Published online: 14 March 2017

Abstract A novel class of quaternary ammonium-based cationic surfactants is synthesized and characterized via spectroscopic methods (FTIR, ^{1}H NMR and ^{13}C NMR). The surface properties, foaming power and biodegradability of the synthesized cationic surfactants are determined using the surface tension technique. The protection performance with their adsorption mechanisms for carbon steel is evaluated in a 15% HCl solution by a series of techniques including electrochemical impedance spectroscopy, potentiodynamic polarization curves, scanning electron microscopy (SEM), X-ray spectroscopy, and UV–visible spectroscopy. The surfactants are found to be excellent corrosion inhibitors for carbon steel. The results show that the inhibition efficiencies are increased by increasing the concentration and the hydrophobic chain length of the tested compounds reaching the maximum at 250 ppm. The potentiodynamic polarization curves suggested that the inhibitors behave as a mixed type with predominant cathodic inhibition and the corrosion behavior can be explained by the adsorption film mechanism. Moreover, the mode of adsorption obeys the Langmuir adsorption isotherm; also, the adsorbed layer on the surface of the metal is approved by using SEM.

Keywords Cationic surfactants · Corrosion inhibition · Carbon steel · Cyclohexene · EIS · SEM · EDX

Introduction

Carbon steel is widely used in different engineering and industrial applications, including designs and construction, where it is deployed in various service environments containing aggressive solutions [1]. In industrial applications, 15% HCl and 20% H_2SO_4 are employed for scale removal treatments and chemical and electrochemical etching of metals [2, 3]. To control the aggressive attack of acid solution on tubing, casing materials (C steel) and other metallic surfaces, inhibitors are added to the acid solution during the acidifying process [4, 5].

The impact of the inhibitor upon the corrosion of metals is predominantly correlated with chemical or physical adsorption. This phenomenon is due to the occurrence of hetero atoms as well as multiple bonds or aromatic rings in the compound chemical structure [6]. It has been reported that during the acidizing procedure, a variety of organic compounds act as corrosion inhibitors for steel, such as alkenylphenones [7–9], amides, nitrogen-containing heterocycles [10], pyridine and its derivatives or salts, nitriles, imminium salts, thiourea derivatives, triazoles, quinoline derivatives, thiosemicarbazide, quaternary salts, thiocyanates [11, 12], and surfactants [1, 13–15].

The surfactant inhibitors have many advantages including a low price, low toxicity, easy production, and high inhibition efficiency [16]. The majority of cationic surfactants are based on the nitrogen atom carrying the cationic charge.

Electronic supplementary material The online version of this article (doi:10.1007/s11743-017-1947-7) contains supplementary material, which is available to authorized users.

✉ Hany M. Abd El-Lateef
Hany_shubra@yahoo.co.uk

Ahmed H. Tantawy
daht1982@yahoo.com

[1] Chemistry Department, Faculty of Science, Sohag University, Sohag 82524, Egypt

[2] Chemistry Department, Faculty of Science, Benha University, Benha, Egypt

Quaternary ammonium-based cationic surfactants are considered as having the most potential for corrosion control, especially on the carbon steel materials in acidic media [17]. Different quaternary ammonium salts have been studied, such as 3-methylbenzo[d]thiazol-3-ium bromide [18], cetylpyridinium chloride (CPC) [19], cetyl trimethyl ammonium bromide [20], and decyldimethylisopropylammonium-hydroxide [21]. The corrosion resisting property of the metal can be markedly changed by the adsorption of the surfactant on the electrode surface. Therefore, the study of the relationship between adsorption and the corrosion inhibition is of great significance [22–24]. The corrosion inhibition of Fe (purity 99.5%) by some 2-(alkyl dimethylamonio) butanol bromide surfactants ($n = 11$–15) was investigated by Elachouri *et al*. [25]. They found that the inhibition efficiency was directly proportional to the number of carbon atoms in the side chain and to the surfactant concentration. Hamitouche *et al.* [26] synthesized quaternary ammonium surfactant mixtures based on a petroleum fraction and tested them as corrosion inhibitors for carbon steel in 1.0 M HCl at 25 °C. The results showed that these surfactants are effective in preventing corrosion and their inhibition efficiency improved with increasing surfactant dose (its optimal value of 70% was for a surfactant concentration of 320 ppm).

In this study, new water-soluble quaternary ammonium-based cationic surfactants were synthesized and their chemical configurations were elucidated and confirmed using different analytical tools including Fourier transform infrared (FTIR) analysis, and ^{1}H and ^{13}C nuclear magnetic resonance (NMR). The inhibition performance of synthesized surfactants on carbon steel pipelines in 15% HCl solution was examined. The study is carried out through potentiodynamic polarization curves and electrochemical impedance spectroscopy (EIS) methods. The thermodynamic parameters of adsorption of the inhibitor are calculated to clarify how the inhibitor works. The surfaces of the samples after immersion tests are analyzed by scanning electron microscopy with energy dispersive X-ray analysis (SEM/EDX).

Experimental Techniques

Materials

Octadecyl, hexadecyl and dodecylamines were obtained from Across Chemical Company (UK). O-chlorobenzaldehyde and acetylacetone were purchased from Sigma-Aldrich Pvt. Ltd., India. Absolute ethanol and triethylamine were purchased from El Goumhoria Trade Pharmaceuticals and Chemicals Company, Cairo, Egypt, while dimethyl sulphate, diethyl ether and tetrahydrofuran were obtained from M/s S.D. Fine Chemicals Pvt., Ltd., India with the highest purity available and were used without any further treatment.

The cylindrical carbon steel of type C1018 which was used in this study has the following chemical composition (wt.%): C 0.17%, Si 0.17%, Ni 0.01%, Mn 0.70%, S 0.03%, Cr 0.01% and the rest is Fe.

The testing media, aqueous aerated 15% HCl, was prepared by dilution of 37% HCl (analytical grade) with doubly distilled water. The concentration of the synthesized surfactant inhibitors which were used ranged from 50 to 250 ppm by weight. All solutions were prepared using bi-distilled water.

Instrumentation

Melting points of obtained compounds were determined using a GallenKamp instrument. NMR spectra were measured and recorded in the Central Lab., Chemistry Department, Faculty of Science, Sohag University at 25 °C on a multinuclear FT-NMR spectrometer Bruker ARX400 at 400.1 (^{1}H) and 100.6 (^{13}C and dept) MHz. The ^{1}H and ^{13}C NMR chemical shifts δ are given in ppm. The FTIR spectrum is recorded in KBr on a thermo Nicolet iS10 FTIR spectrophotometer. The surface tension of aqueous solutions was measured by a Tensiometer – K6 processor (KRÜSS company, Germany) using the ring method, and each sample result was determined from the average of three measurements.

Synthesis of the Quaternary Ammonium Surfactants (3a–c)

The synthesis of target cationic surfactants was performed in two main steps as shown in Fig. 1.

Synthesis of Cyclohexene Derivatives Based on Fatty Amines by Conventional Heat

A solution of 20 mol of fatty amines was added to a heated mixture of 60 mol of acetylacetone and 20 mol of O-chlorobenzaldehyde in 50 ml of ethanol in the presence of two drops of triethylamine as a base catalyst. The reaction mixture was refluxed for 4–5 h at 90 °C and left to cool down to room temperature. A precipitate was obtained, filtered and washed with cold ethanol. The solid products were recrystallized from ethanol to afford the products 2a–c.

Synthesis of Novel Cationic Surfactants (3a, 3b and 3c)

In a single-neck flask, 20 mol of the synthesized cyclohexenes derivatives 2a–c were reacted separately with

60 mol of dimethyl sulphate in tetrahydrofuran as a solvent for 48 h at room temperature. Solid products were obtained, filtered, recrystallized from diethyl ether and dried to afford the required cationic surfactants 3a–c. The chemical structure of the synthesized compounds was established by FTIR, ^{1}H and ^{13}C NMR spectra.

Electrochemical Measurements

All the corrosion measurements under unstirred conditions were recorded using Versa STAT4 potentiostat/galvanostat in a three-electrode conventional electrolytic cell consisted of: C1018 carbon steel with a diameter of 0.5 cm, length of 3.0 cm, 4.55 cm^{2} of exposed area as the working electrode (WE), a saturated calomel electrode (SCE) as the reference and a platinum wire as a counter electrode. The polarization studies were carried out at potential range of ± 250 mV with respect to the open circuit potential (E_{corr}) and at a sweep rate of 1.0 mV s^{-1}.

EIS measurements were performed with a phase-sensitive amplifier (model 5208) driven through a potentiostat/galvano stat Versa STAT4 with a frequency response analyzer (FRA) connected with a computer control. EIS was carried out at E_{corr} after 60 min of immersion in a frequency range of 10 kHz–0.5 Hz by applying 10 steps per frequency decade. The impedance parameters were calculated from the EIS measurements by fitting the obtained results to the equivalent circuit model using the fit and simulation tool of the Z-View software. It is well-known that the corrosion rate of carbon steel depends on temperature, whereas the largest value was recorded at 50 °C [27]. Therefore, in order to accurately estimate the inhibition performance of the synthesized surfactants on carbon steel substrate in 15% HCl solution, all the experiments were performed at 50 °C.

Surface Tension Measurements

The surface tension measurements were performed for different aqueous solutions of the synthesized cationic surfactants in water and 15% HCl at 30 °C. The prepared solutions were poured into clean Teflon containers and left for 1 h to allow stabilization and complete adsorption at the solution surface. The values of surface tension were measured a minimum of three times and the recorded values were taken as the average of these values. The critical micelle concentration (CMC) and some surface indices were calculated.

Foaming Power and Biodegradability

Measurements of foam power were done after shaking 100 mL of 0.1% concentration of the synthesized cationic surfactant solution vigorously in a closed, graduated, 250-mL cylinder at 30 °C. Foam formation was measured by the foam height (in ml) initially produced, and foam stability was recorded by the time [28]. The biodegradability was measured according to the previous work [29].

UV–Visible Spectroscopy

The UV–visible spectrophotometric measurements were achieved via a JASCO UV–visible spectrophotometer and a 10-mm matched silica cell.

Surface Characterization by SEM, EDX and FTIR

In order to observe any changes in surface morphologies of the carbon steel samples after testing, the specimens were first immersed in 15% HCl solution with and without 250 ppm of investigated surfactants for 2 days, then washed with bi-distilled water and acetone, and dried with cool air. The morphology of the surface of tested samples was observed by using SEM with a 3.0-kV operating voltage equipped with an EDX detector (JEOL, model 5300). Moreover, the specimens were taken out and dried. Then, the nature of the film formed on the metal surface was analyzed by FTIR.

Results and discussion

Spectroscopic Analysis of the Prepared Compounds

The spectroscopic data of the prepared compounds are shown as follows:

5-N-(dodecyl)amino-2,4-diacetyl-1-methyl-3-(2-chlorophenyl)-4-cyclohexen-1-ol ***[2a]***

Darkish red color, semisolid, yield = 87%. FTIR (KBr pellet, cm^{-1}): 3110–3343(OH), 3210 (NH), 3039 (C–H arom.) 2952, 2930, and 2856 (C–H, aliphatic fatty chain), 1707(C=O), and 1589 (C=C arom.; supporting data, Fig. S1a).

^{1}H NMR (400 MHz) δ (ppm; DMSO-d_6): 0.98 (*t*, 3H, $\mathbf{CH_3}$–CH$_2$–), 1.13 (s, 3H, $\mathbf{CH_3}$–C–OH), 1.24 (s, 20 H, $\mathbf{(CH_2)_{10}}$–), 1.50 (t, 2H, $\mathbf{CH_2}$–NH), 2 (s, 6H, 2$\mathbf{CH_3}$–C=O), 2.64 (d, 1H, **CH**-C=O cyclic), 3.33 (s, 2H, $\mathbf{CH_2}$ cyclic), 4.23 (d, J = 8 Hz, 1H, **CH**-Ar cyclic), 4.51 (s, 1H, C–**OH**), 7.18–7.48 (m, J = 8 Hz, 4H, **CH** arom.), 11.58 (broad, 1H, **NH**; supporting data, Fig. S1b).

^{13}C NMR (100 MHz) δ (ppm; DMSO-d_6): 14.28 [$\mathbf{CH_3}$-alkyl chain], 14.38 [**CH**–C=O cyclic], 22.55 [–**CH**–Ar cyclic], 26.70 [–$\mathbf{CH_2}$–CH$_2$NH–], 28.93 ($\mathbf{CH_3}$–C–OH), 29.44 [9(–$\mathbf{CH_2}$–) alkyl chain], 31.78 [2($\mathbf{CH_3}$–C=O)], 42.26

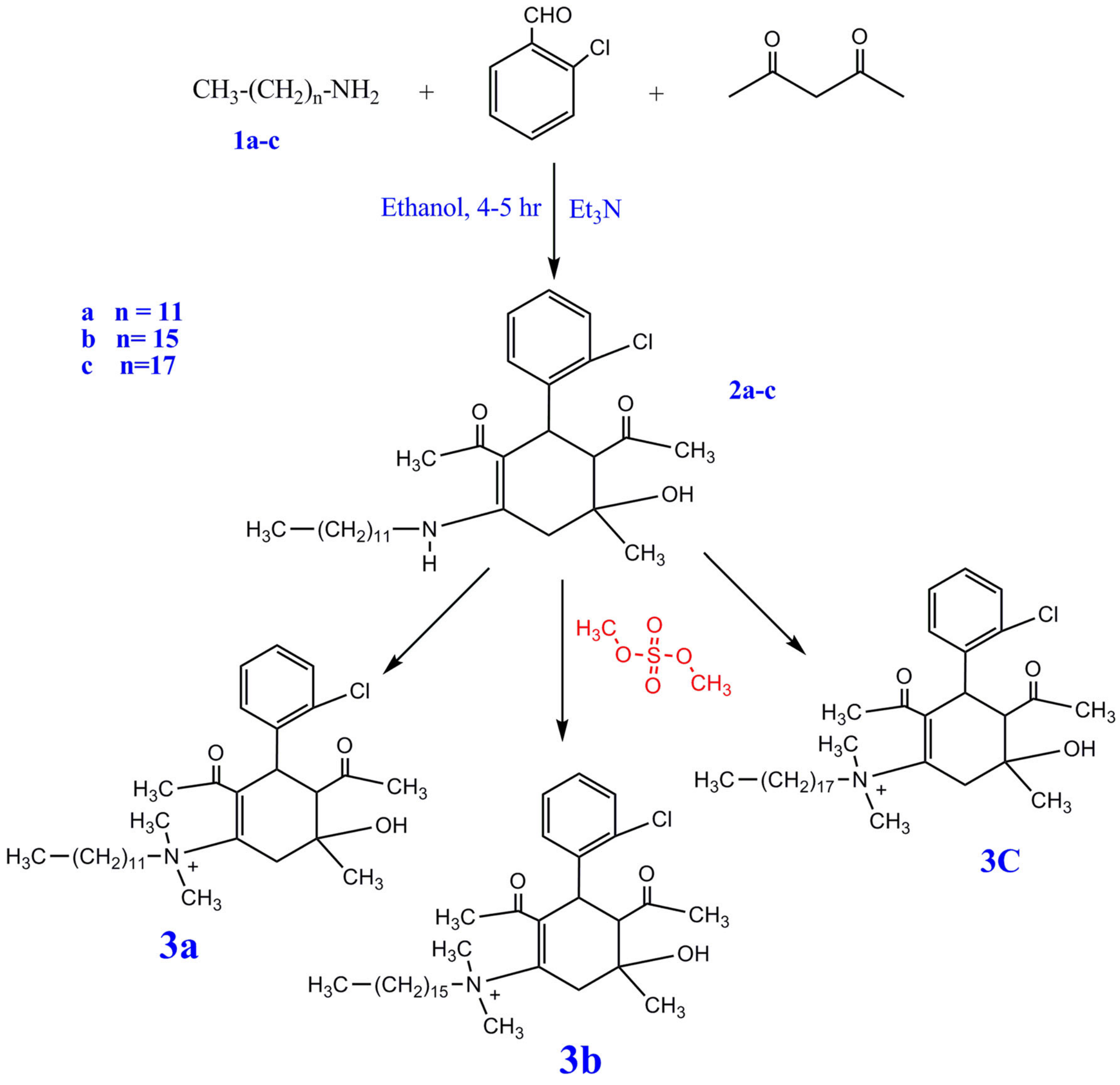

Fig. 1 Synthesis procedure of the investigated cationic surfactants (3a, 3b and 3c)

[–**CH$_2$**–NH], 64.31 [**C**–OH], 68.21 [**CH$_2$**–C–OH)], 94.87 [**C**=C–], 127.83–144.34 [**6C**, arom.], 163.44 [NH–**C**=C], 194.13, 196.16 [2**C**=O] (supporting data, Fig. S1c).

*5-N-(hexadecyl)amino-2,4-diacetyl-1-methyl-3-(2-chlorophenyl)-4-cyclohexen-1-ol [**2b**]*

Yellow color, solid, mp = 101–105 °C, yield = 83%. FTIR (KBr pellet, cm^{-1}): 3095–3300 (OH), 3250 (NH), 3031 (C–H arom.), 2918 and 2850 (C–H, aliphatic fatty chain), 1693 (C=O), and 1602 (C=C arom.).

^{1}H NMR (400 MHz) δ (ppm; DMSO-d_6): 0.86 (t, 3H, **CH$_3$**–CH$_2$–), 1.13 (s, 3H, **CH$_3$**–C–OH), 1.26 (s, 28H, (**CH$_2$**)$_{14}$–), 1.55 (t, 2H, **CH$_2$**–NH), 1.89 (s, 6H, **2CH$_3$**–C=O), 2.24 (d, 1H, **CH**–C=O cyclic), 3.21 (s, 2H, **CH$_2$** cyclic), 4.48 (d, J = 8 Hz, 1H, **CH**–Ar cyclic), 5.04 (s, 1H, C–**OH**), 7.11–7.77 (m, J = 8 Hz, 4H, **CH** arom.), 11.78 (broad, 1H, **NH**; supporting data, Fig. S2a).

^{13}C NMR (100 MHz) δ (ppm; DMSO-d_6): 14.11 [$\underline{CH_3}$-alkyl chain], 23.65 [–**CH**–C=O cyclic], 27.12 [**CH$_2$**–CH$_3$], 27.48 [–**CH$_2$**–CH$_2$NH–], 29.11 [**CH$_3$**–C–OH], 29.43 [12(–**CH$_2$**–) alkyl chain], 32.16 [Ar–**CH**–C=C], 42.11 [2(**CH$_3$**–C=O)], 44.24 [**CH$_2$**–NH], 65.22 [**C**–OH], 68.11 [**CH$_2$**–C–OH], 114 [**C**=C–], 127–130 [$\underline{6C}$, arom.], 160.43 [NH–**C**=C], 194.44, 211.43 [2**C**=O] (supporting data, Fig. S2b).

*5-N-(1-octadecyl)amino-2,4-diacetyl-1-methyl-3-(2-chlorophenyl)-4-cyclohexen-1-ol [**2c**]*

White color, solid, mp = 106–112 °C, Yield = 85%. FTIR (KBr pellet, cm^{-1}): 3100–3200 (OH), 3300 (NH), 3039 (C–H arom.), 2952, 2930, and 2856 (C–H, aliphatic fatty chain), 1703 (C=O), and 1589 (C=C arom.).

^{1}H NMR (400 MHz) δ (ppm; DMSO-d_6): 0.86 (t, 3H, $\mathbf{CH_3}$–CH_2–), 1.13 (s, 3H, $\mathbf{CH_3}$–C–OH), 1.24 (s, 32H, $(\mathbf{CH_2})_{\mathbf{16}}$–), 1.51 (t, 2H, $\mathbf{CH_2}$–NH), 2.05 (s, 6H, 2$\mathbf{CH_3}$–C=O), 2.51 (d, 1H, **CH**–C=O cyclic), 3.11 (s, 2H, $\mathbf{CH_2}$ cyclic), 4.21 (d, J = 8 Hz, 1H, **CH**–Ar cyclic), 4.63 (s, 1H, C–**OH**), 7.08–7.51 (m, J = 20 Hz,4H, **CH** arom.), 11.66 (s. br., 1H, **NH**; supporting data, Fig. S3a).

^{13}C NMR (100 MHz) δ (ppm; DMSO-d_6): 14.30 [$\mathbf{CH_3}$-alkyl chain], 22.48 [–**CH**–C=O], 28.59 [$\mathbf{CH_3}$–C–OH], 29.11 [–$\underline{CH_2}$–CH_2NH–], 29.43 [15(–$\mathbf{CH_2}$–) alkyl chain], 31.99 [–**CH**–Ar cyclic], 41.02 [2($\mathbf{CH_3}$–C=O)], 43.68 [–$\mathbf{CH_2}$–NH], 66.29 [**C**–OH], 67.11 [$\mathbf{CH_2}$–C–OH)], 103.35 [C=C–], 126.22–130.71 [**6C**, arom.], 159.81 [NH–C=C], 194.93, 211.12 [**2C**=O] (supporting data, Fig. S3b).

*N-(2,4-diacetyl-1-methyl-3-(2-chlorophenyl)-4-cyclohexen-1-ol)-N,N,N-dimethyl, dodecyl ammonium salt [**3a**]*

Darkish violet color, viscous, yield = 85%. FTIR (KBr pellet, cm^{-1}): 3100–3430 (OH), 3034 (C–H arom.) 2951, 2932, and 2851 (C–H, aliphatic fatty chain), 1703 (C=O), and 1595 (C=C arom.).

^{1}H NMR (400 MHz) δ (ppm; DMSO-d_6): 0.58 (t, 6H, $\mathbf{CH_3}$–CH_2–), 0.82 (s, 3H, $\mathbf{CH_3}$–C–OH), 0.98 (s, 20H, $(\mathbf{CH_2})_{\mathbf{0}}$–), 1.30 (s, 6H, 2$\mathbf{CH_3}$–C=O), 1.88 (s, 2H, $\mathbf{CH_2}$–C=C), 2.26 (d, H, **CH**–Ar), 2.85 (d, 1H, **CH**–C=O), 2.95 (s, 1H, C–**OH**), 4.77 [s, 8H, $(\mathbf{CH_3})_2$–$N^+\underline{\mathbf{CH_2}}$] 7.01–7.66 (m, 4H, **CH** arom.) and disappear the NH band (supporting data, Fig. S4a).

^{13}C NMR (100 MHz) δ (ppm; DMSO-d_6): 14.17[$\mathbf{CH_3}$-alkyl chain], 22.39 [–**CH**–C=O cyclic], 25.43 [–$\mathbf{CH_2}$–CH_3], 26.22 [–$\mathbf{CH_2}$–CH_2N^+–], 28.22 [$\mathbf{CH_3}$–C–OH], 29.30 [8(–$\mathbf{CH_2}$–) alkyl chain], 31.64 [–**CH**–Ar cyclic], 46.70 [$\mathbf{CH_2}$–C–OH cyclic], 58.10 [$(\mathbf{CH_3})_2$–N^+–$\mathbf{CH_2}$)], 65.24 [**C**–OH], 96.11 [**C**=C–], 98 [C=**C**–], 128–132 [**4C**, arom.], 198.21 [2$\underline{C}$=O] (supporting data, Fig. S4b).

*N-(2,4-diacetyl-1-methyl-3-(2-chlorophenyl)-4-cyclohexen-1-ol)-N,N,N-dimethyl, hexadecyl ammonium salt [**3b**]*

Darkish red color, viscous, yield = 90%. FTIR (KBr pellet, cm^{-1}): 3111–3420 (OH), 3104 (C–H arom.) 2956, 2930, and 2831 (C–H, aliphatic fatty chain), 1707 (C=O), and 1600 (C=C arom.).

^{1}H NMR (400 MHz) δ (ppm; DMSO-d_6): 0.67 (t, 6H, $\mathbf{CH_3}$–CH_2–), 0.83 (s, 3H, $\mathbf{CH_3}$–C–OH), 1.00 [m, 28H, $(\mathbf{CH_2})_{\mathbf{14}}$–], 1.15 (s, 6H, 2$\mathbf{CH_3}$–C=O), 1.86 (s, 2H, $\mathbf{CH_2}$–C=C), 2.27 (d, H, **CH**–C–OH), 2.98 (d, 1H, **CH**–Ar cyclic), 3.31 (s, 1H, C–**OH**), 4.51 (s, 8H, $(\mathbf{CH_3})_2$–$N^+\underline{CH_2}$) 7.01–7.50 (m, 4H, **CH** arom.) and disappear the **NH** band.

^{13}C NMR (100 MHz) δ (ppm; DMSO-d_6): 12.16 [$\mathbf{CH_3}$-alkyl chain], 21.40 [–**CH**–C=O cyclic], 21.43 [–$\mathbf{CH_2}$–CH_3], 26.00 [–$\mathbf{CH_2}$–CH_2N^+–], 27.02 ($\mathbf{CH_3}$–C–OH), 29.47 [12(–$\mathbf{CH_2}$–) alkyl chain], 35.64 [Ar–**CH**– cyclic], 41.71 [$\mathbf{CH_2}$–C–OH cyclic], 59.11 [$(\mathbf{CH_3})_2$–N^+–$\underline{CH_2}$)], 66.54 [**C**–OH], 96.59 [**C**=C], 99.11 [C=**C**–], 127–132 [**6C**, arom.], 210.21 [2**C**=O].

*N-(2,4-diacetyl-1-methyl-3-(2-chlorophenyl)-4-cyclohexen-1-ol)-N,N,N-dimethyl, octadecyl ammonium salt [**3c**]*

Deep orange color, viscous, yield = 92%. FTIR (KBr pellet, cm^{-1}): 3150–3400 (OH), 3101 (C–H arom.) 2956, 2930, and 2831 (C–H, aliphatic fatty chain), 1701 (C=O), and 1600 (C=C arom.).

^{1}H NMR (400 MHz) δ (ppm; DMSO-d_6): 0.62 (t, 6H, $\mathbf{CH_3}$–CH_2–), 0.79 (s, 3H, $\mathbf{CH_3}$–C–OH), 1.21 [m, 32H, $(\mathbf{CH_2})_{\mathbf{16}}$–], 1.11 (s, 6H, 2$\mathbf{CH_3}$–C=O), 1.76 (s, 2H, $\mathbf{CH_2}$–C=C), 2.17 (d, H, **CH**–C–OH), 2.98 (d, 1H, **CH**–Ar cyclic), 3.30 (s, 1H, C–**OH**), 4.01 (s, 8H, $(\mathbf{CH_3})_2$–$N^+\mathbf{CH_2}$) 7.23–7.51 (m, 4H, CH arom.) and disappear the NH band.

^{13}C NMR (100 MHz) δ (ppm; DMSO-d_6): 11.18 [$\mathbf{CH_3}$-alkyl chain], 20.45 [–**CH**–C=O cyclic], 25.22 [–$\mathbf{CH_2}$–CH_3], 26.63 [–$\mathbf{CH_2}$–CH_2N^+–], 26.02 ($\mathbf{CH_3}$–C–OH), 28.46 [14(–$\mathbf{CH_2}$–) alkyl chain], 31.64 [–**CH**–Ar cyclic], 48.71 [$\mathbf{CH_2}$–C–OH)], 59.12 [$(\mathbf{CH_3})_2$–N^+–$\mathbf{CH_2}$)], 66.23 [**C**–OH], 98.23 [**C**=C], 101.13 [C=**C**–], 131–135 [**6C**, arom.], 209.22 [2**C**=O].

Potentiodynamic Polarization Curves

The cathodic and anodic polarization curves of carbon steel in the absence and presence of various concentrations of the synthesized surfactant inhibitors (3a, 3b and 3c) at 50 °C and a scan rate of 1.0 mV/s are depicted in Fig. 2. It is seen that incorporating of the inhibitor into the corrosive solution causes a marked decrease in the rate of corrosion, i.e., shifts the cathodic curves toward more negative potentials and the anodic curves toward more positive potentials. This may be due to adsorption of the surfactant molecule on the metal substrate [30]. The important related Tafel indices including anodic and cathodic Tafel slopes (β_a, β_c), corrosion potential (E_{corr}) and the corrosion current density (I_{corr}) were determined from the polarization plot and are tabulated in Table 1. The E_{corr} can be calculated by extrapolation of the anodic and cathodic Tafel lines slope [31–33]. The inhibition efficiency ($P\%$) and the surface coverage (θ) were calculated from the following equations [34]:

$$\theta = \frac{(I_{\mathrm{corr}})_{uninh} - (I_{\mathrm{corr}})_{\mathrm{inh.}}}{(I_{\mathrm{corr}})_{\mathrm{uninh}}} \quad (1)$$

$$P\% = \theta \times 100 \quad (2)$$

where $(I_{\mathrm{corr}})_{\mathrm{uninh}}$ and $(I_{\mathrm{corr}})_{\mathrm{inh}}$ are the corrosion current densities in the absence and presence of the surfactant inhibitors, respectively.

The results in Table 1 show that the presence of inhibitors led to the value of E_{corr} shifting towards a more negative direction, which can be explained by a predominance of the cathodic reaction inhibition. The investigated surfactants can be classified as a cathodic or anodic type inhibitor when the changing in the E_{corr} value is greater than 85 mV [35]. The largest displacements exhibited by 3a, 3b and 3c were 16, 22 and 18 mV, respectively at 50 °C (Table 1), which indicated that these molecules should be considered a mixed-type inhibitors, meaning that the addition of cationic surfactants to the investigated acid solution both decreases the anodic dissolution of steel and delays the cathodic hydrogen evolution reaction. Figure 2 shows that the cathodic and anodic current density are directly proportional with concentrations of the surfactant inhibitors. This behavior can be explained by the adsorption of the inhibitor molecules on the steel surface, forming a protective layer.

As shown in Table 1, the corrosion current density (I_{corr}) became lower and the inhibition efficiency ($P\%$) increases with increments of the surfactant concentrations, noting that these inhibitors served as effective inhibitors for carbon steel in the aggressive hydrochloric acid solution. This can be interpreted based on the adsorption of inhibitor on the steel substrate and the adsorption process being strengthened by the increase in the inhibitor concentration. The inhibition performance of the investigated compounds was dependent on the inhibitor structure (the length of hydrophobic chain) and concentration.

Based on Fig. 2 and Table 1, it was found that the anodic Tafel slope (β_a) and cathodic Tafel slope (β_c) values in the blank 15% HCl solutions are higher than those in presence of the inhibitors. This indicates that the corrosion reaction has stronger influence in the absence of inhibitors [36]. This is because the Tafel slopes (β_a and β_c) of the studied inhibitors were found to change with surfactant concentrations. This indicates that these inhibitors affect both anodic dissolution of steel and hydrogen evolution reaction [37]. In addition, the values of β_c in the absence and presence of investigated inhibitors are higher than 118 mV/dec. It indicates that the corrosion reaction proceeded mainly by charge transfer and substance diffusion [1]. The values of β_c show a slight change with increasing surfactant dose, indicating the influence of these compounds on the kinetics of hydrogen evolution. This may probably be due to a diffusion or barrier effect [32]. In this case, the dissolution reaction of iron ($Fe \rightarrow Fe^{2+} + 2e^-$) is balanced by the cathodic reaction on the adjacent surface ($2H^+ + 2e^- \rightarrow 2H_{ad} \rightarrow H_2$). Accordingly, the hydrogen evolution and mass loss is produced by the reaction ($Fe + 2H^+ = Fe^{2+} + H_2$) [38].

The data in Table 1 indicate that the values of surface coverage (θ) near unity indicate nearly a whole coverage of the steel surface with adsorbed inhibitor molecules. Conclusively, the high θ value is evaluated as a good physical bulkhead shielding the corroding surface from corrosive acid solution and decreasing the corrosion rate of steel dramatically. Finally, it can be concluded that the high values of $P\%$ are related to the high θ values of the surfactant molecules. It is clear that $P\%$ increases with increase in surfactant dose with the highest value of 89.66, 95.13 and 97.21 for 3a, 3b and 3c, respectively, obtained at 250 ppm of the inhibitors. The order of $P\%$ of the inhibitors at various concentrations as given by potentiodynamic measurements is 3c > 3b > 3a. This order will be discussed later in the corrosion inhibition mechanism.

Electrochemical impedance spectroscopy (EIS) measurements

The Nyquist plots obtained from the EIS measurements at an open-circuit potential for carbon steel in 15% HCl solutions in the absence and presence of different concentrations of surfactants (3a, 3b and 3c) are presented in Fig. 3a–c. It is evident that the curves were described by a semicircle and a single relaxation process (one time constant), which means the process was mainly controlled by capacitance; this can be interpreted as the formation of a protective adsorption film at the steel/solution interface [39]. The capacitive semicircle is attributed to charge transfer resistance (R_{ct}) and the double-layer capacitance (C_{dl}). The R_{ct} values were measured from the difference in impedance at higher and lower frequencies [40]. It is observed from Fig. 3a–c that the semicircles have different size; the semicircle is small in the case of free acid solution and the introduction of surfactants to the aggressive medium. The magnitude of the semicircle loops increases as the inhibitor dose increases; hence, the inhibition performance is promoted due to the adsorption of surfactant molecules to the steel substrate [41]. The Nyquist diagrams were fitted using the Z-view program and the impedance parameters were calculated from fitting results using the best equivalent electrical circuit which is commonly used. Figure 4 shows the equivalent model circuit used to accurately fit the obtained results for carbon steel in 15% HCl in the absence and presence of the investigated inhibitors. In this circuit, R_s corresponds to solution resistance, R_{ct}

Fig. 2 Potentiodynamic polarization curves for carbon steel in 15% HCl solution at 50 °C containing various concentrations of (**a**) 3a, (**b**) 3b and (**c**) 3c compounds

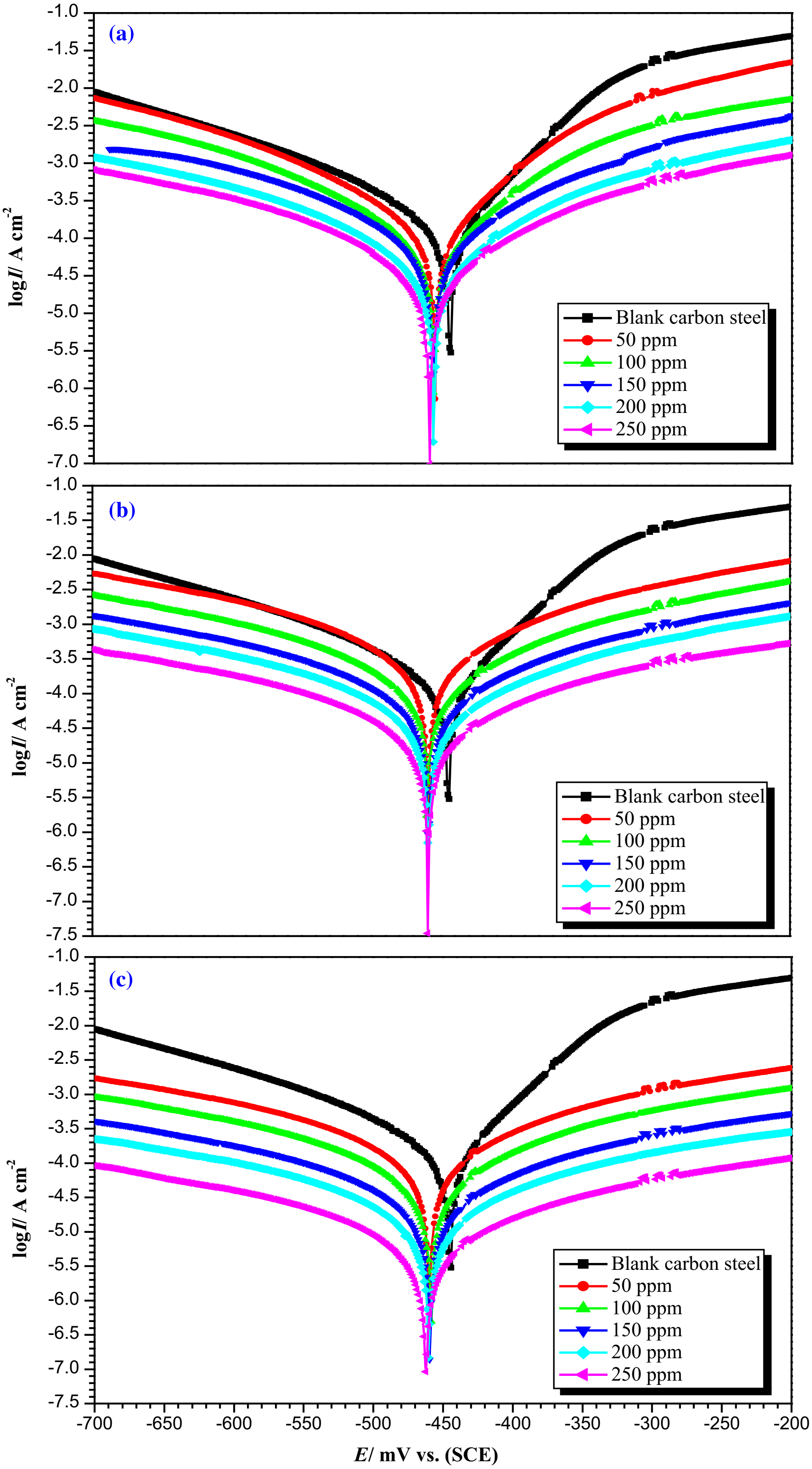

Table 1 Polarization parameters for carbon steel in 15% HCl solution at 50 °C with various concentrations of studied surfactants

Compounds	C_{inh} (ppm) by weight	I_{corr} (mAcm^{-2})	$-E_{corr}$ (mV vs. SCE)	β_a/mV (dec^{-1})	$-\beta_c$ (mV dec^{-1})	θ	P (%)
Blank	0.0	14.71	444	94	178	–	–
3a	50	9.34	456	78	150	0.365	36.5
	100	6.65	457	75	161	0.547	54.7
	150	5.33	459	71	164	0.637	63.7
	200	3.79	457	76	142	0.742	74.2
	250	1.52	460	80	156	0.896	89.6
3b	50	8.78	459	73	163	0.402	40.2
	100	5.97	460	76	157	0.593	59.3
	150	4.29	458	71	152	0.707	70.7
	200	2.68	466	78	154	0.817	81.7
	250	0.71	455	81	156	0.951	95.1
3c	50	8.01	458	76	165	0.455	45.5
	100	5.42	457	74	149	0.631	63.1
	150	3.74	460	78	157	0.745	74.5
	200	2.02	455	72	159	0.862	86.2
	250	0.41	464	74	163	0.972	97.2

corresponds to charge transfer resistance and Q_{CPE} to the constant phase elements for the double layer. A similar equivalent circuit was proposed by Zhang *et al.* [42] for the corrosion inhibition of mild steel in HCl solution by quaternary ammonium salt derivatives. The steel/solution interface does not behave like an ideal capacitor. Other than this, the constant phase element (Q_{CPE}) is replaced a double layer capacitance (C_{dl}) to recompense for non-ideal capacitive response of the interface and to obtain a more careful fit of the experimental results set [43]. The CPE-type impedance, Q_{CPE}, was calculated from the following equation [44]:

$$Q_{CPE} = \frac{1}{Y_0(J)^n} \tag{3}$$

where Y_o is a proportional factor, ω is the angular frequency $= 2\pi f$ and n is the phase shift, which gives information about the degree of non-ideality in capacitive behavior. For $n = 0$, Q_{CPE} represents a pure resistance, for $n = 1$ a capacitance, for $n = 0.5$ a Warburg impedance and for $n = -1$ an inductive. The lower value of n (0.76) for carbon steel in 15% HCl indicated surface inhomogeneity resulted from roughening of the steel surface due to corrosion. Addition of 3a, 3b and 3c inhibitors (250 ppm) to the aggressive solution increased the n value from 0.74 to 0.86, 0.89 and 93, respectively, indicating lessening of surface inhomogeneity due to the adsorption of surfactant molecules.

Figures S5 and S6 in the supporting data show Bode and phase angle plots for carbon steel electrode immersed in 15% HCl in the absence and presence of various concentrations of inhibitors. As seen from Fig. S5 (supporting data), Bode plots point to the presence of an equivalent circuit that contains a single constant phase element in the steel/medium interface. The linear relationship between log|Z| vs. log f with a slope (α) near -1 ($\alpha = -0.84, -0.86$ and -0.89 in the presence of 250 ppm of 3a, 3b and 3c compounds, respectively) could be associated to the non-ideal structure of the steel/acid interface. In regard to this matter, a differential capacitance should be formed at the interface instead of an ideal capacitor. Figure S6 (supporting data) shows the phase angle plots of the synthesized inhibitors. As we can see, increasing the inhibitor dose in the studied acid medium results in the phase angle being closer to 90 degrees, indicating superior inhibitive behavior due to adsorption of more inhibitor molecules on the metal surface at higher concentrations [45].

In the case of the EIS, the inhibition efficiency was determined using charge transfer resistance according to the following equation [33]:

$$P\% = \frac{(R_{ct})_{inh} - (R_{ct(0)})_{uninh}}{(R_{ct})_{inh}} \times 100 \tag{4}$$

where $(R_{ct})_{inh}$ and $(R_{ct(0)})_{uninh}$ indicate the values of the charge transfer resistances in the presence and absence of inhibitors, respectively. The EIS parameters are listed in Table 2. It is seen on Table 2 that Q_{CPE} values decrease with increasing the inhibitor concentration, which may be attributed to increasing the thickness of the metal/solution interface and/or decreasing the local dielectric constant [46]. Formation of an inhibitor layer increases with an increasing concentration of inhibitors, as more surfactant molecules are adsorbed on the steel surface. Also, the inhibitor molecules may reduce the capacitance by

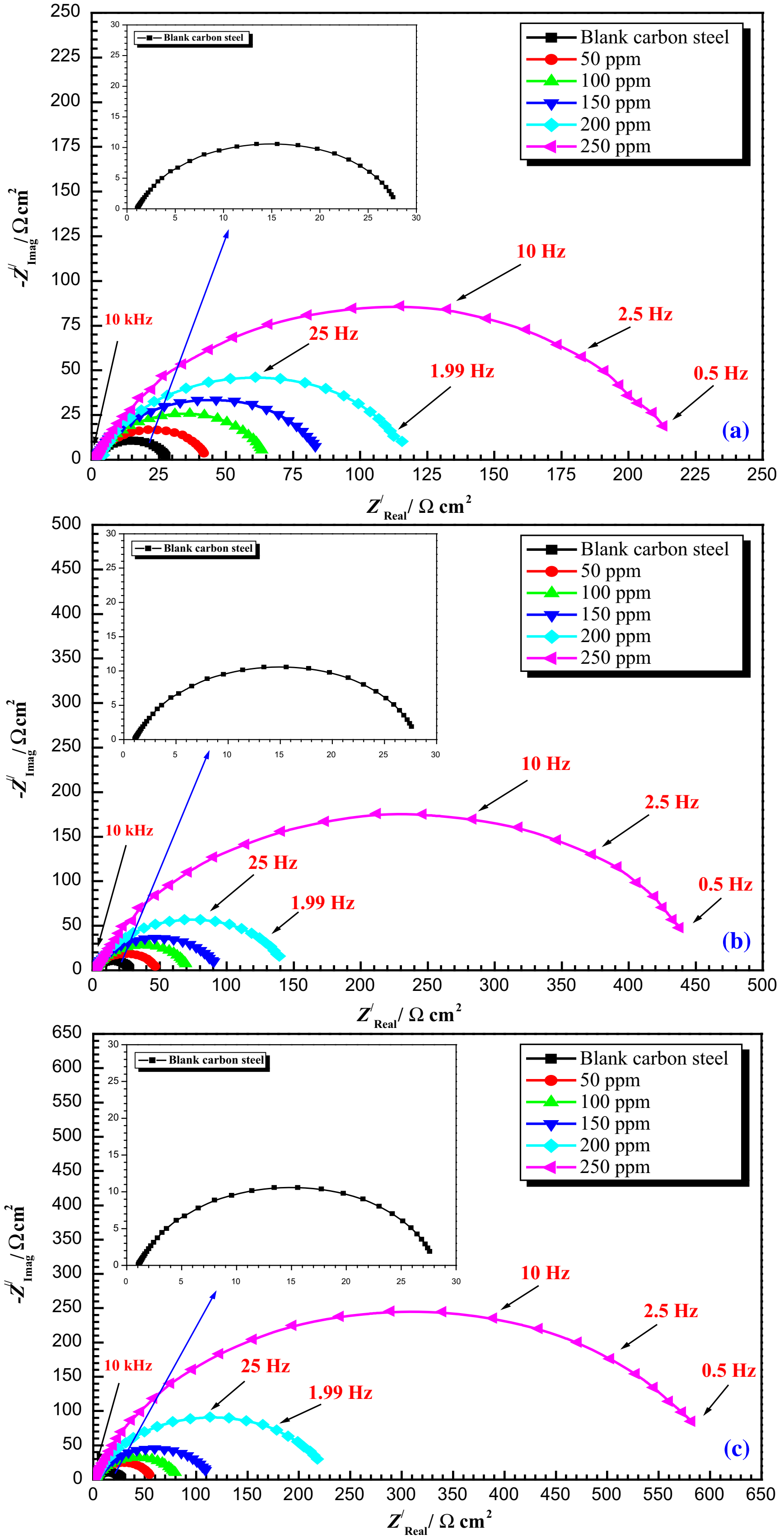

Fig. 3 Nyquist plots for carbon steel in 15% HCl solution at 50 °C in the absence and presence of different concentration of (**a**) 3a, (**b**) 3b and (**c**) 3c inhibitors

increasing the double layer thickness according to the Helmholtz model [33]:

$$Q = \frac{\varepsilon\varepsilon_o}{d} A \quad (5)$$

where ε, ε_0, d and A are the dielectric constant of the protective layer, the permittivity of free space, the thickness of the protective layer and the electrode area, respectively. Addition of synthesized inhibitors provides lower Q values, which may be a result of the effective adsorption of the synthesized inhibitor. As is clear from the data presented in Table 2, the inhibition efficiency ($P\%$) and charge transfer resistance (R_{ct}) increase with increasing inhibitor dose, indicating a reduction in the corrosion rate of carbon steel. A high-impedance response was obtained up to 45, 52 and 60 Ω cm^2 in the presence of 50 ppm of 3a, 3b and 3c compounds, respectively, indicating that the protective film inhibits the corrosion on the carbon steel surface. These values increased to 231, 468 and 646 Ω cm^2, respectively, with increasing inhibitor concentrations to 250 ppm because more inhibitor molecules adsorbed onto the steel surface and resulted in a barrier effect. Based on Table 2, the $P\%$ values were found to increase in the following order: 3c > 3b > 3a with values 95.5 > 93.7 > 87.3%, respectively. It is worth noting from Tables 1 and 2 that the inhibition efficiencies obtained from impedance measurements are comparable and run parallel with those obtained from potentiodynamic polarization measurements.

Surface-Active Properties of the Synthesized Cationic Surfactants

In the present study, the surface tension measurements of the synthesized cationic surfactant were estimated in both distilled water and 15% HCl to study the adsorption characteristics at the air/water interface and micellization of the cationic surfactants in bulk solutions either in distilled or acidic aqueous solutions. Figure 5a, b represent the variation of surface tension (γ) versus −log C of the synthesized cationic surfactants 3a–c in water and 15% HCl at 30 °C. The surface tension profile is characterized by two regions. The first one at lower concentrations is characterized by continuous decrease of the γ values, indicating the accumulation of the surfactant molecules at the air/water interface by increasing the concentration. In the second region, the surface tension variation is almost stable by increasing the concentration [47]. Figure 5a shows that the surfactant with longer hydrophobic chain is easier to be adsorbed at the air/water interface than self-assemble in solution. So, as the hydrophobic chain length increases, the CMC value gradually decreases; this leads to the enhancement of the hydrophobic interaction between the longer alkyl chains. Moreover, the values of CMC were reduced in 15% HCl. These data indicated that the prepared cationic surfactants are strongly adsorbed at interfaces in 15% HCl solutions. It is well-known that the micellization, aggregation and adsorption of surfactants are based on the CMC values, which were determined in water and 15% HCl aqueous solution from abrupt changes of the plotted data of surface tension (γ) versus the solute concentration (log C; Fig. 5a, b) and listed in Table 3.

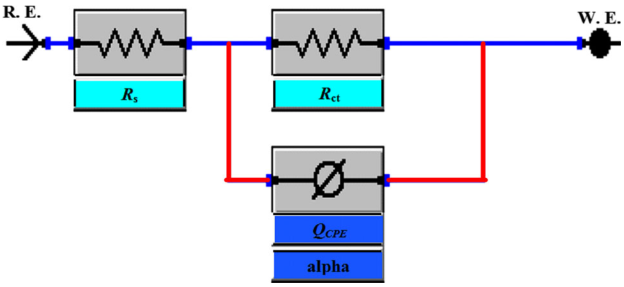

Fig. 4 Electrochemical equivalent circuit used for simulation of impedance spectra

The packing densities of surfactants at the air/water interface are very important to interpret the surface activities of various surfactants. So, the surface activity parameters of 3a–c compounds in water and 15% HCl aqueous solution at 30 °C are listed in Table 3. The maximum surface excess concentration at the air/water interface (Γ_{max}) can be calculated by the Gibbs adsorption isotherm equation [48–50]:

$$\Gamma_{\max} = \frac{1}{2.303nRT}\left(\frac{d\gamma}{d\log C}\right)_T \quad (6)$$

where T is the absolute temperature; R is the gas constant; dγ/dlog$C$ is the slop of γ vs log$C$ profile at the point CMC; and n is a constant and depends on the number of species constituting the surfactant adsorbed at the interface [51]. The minimum area taken by inhibitor molecules at the air/water interface (A_{min}) is calculated by using the Eq. (7) [4]:

$$A_{\min} = \frac{10^{16}}{\Gamma_{\max} \times N_A} \quad (7)$$

where N_A is Avogadro's constant and A_{min} is minimum area per molecule in nm^2. The values of Γ_{max} and A_{min} are listed in Table 3. It is observed from Table 3 that the values of A_{min} in 15% HCl aqueous solution are more than in water. These data indicate that the prepared cationic surfactants favor micellization in bulk 15% HCl solution rather than aqueous solution which may reflect their greater tendency to be adsorbed at the metal/liquid interface is greater than at the air/water interface. Increasing the length

Table 2 Electrochemical impedance parameters for carbon steel in 15% HCl solution in the absence and presence of various concentrations of surfactant inhibitors at 50 °C

Inhibitors code	C_{inh} (ppm) by weight	R_s (Ω cm^2)	R_{ct} (Ω cm^2)	Q_{CPE} (F cm^{-2} $\times$ 10^{-7})	n	θ	P (%)
Absence	0	1.06	29.3	5.43	0.76	–	–
3a	50	1.12	45.1	3.53	0.83	0.351	35.1
	100	1.17	66.6	2.39	0.82	0.561	56.1
	150	1.14	89.3	1.78	0.84	0.672	67.2
	200	1.41	124.4	1.28	0.83	0.764	76.4
	250	1.62	231.6	0.69	0.86	0.873	87.3
3b	50	1.15	52.2	3.05	0.84	0.438	43.8
	100	1.31	74.5	2.13	0.86	0.606	60.6
	150	1.36	98.8	1.61	0.88	0.703	70.3
	200	1.45	155.7	1.02	0.86	0.812	81.2
	250	2.41	468.4	0.34	0.89	0.937	93.7
3c	50	1.29	60.1	2.65	0.86	0.512	51.2
	100	1.34	89.6	1.78	0.91	0.673	67.3
	150	1.66	120.7	1.32	0.91	0.757	75.7
	200	1.90	244.1	0.65	0.92	0.881	88.1
	250	3.11	646.3	0.25	0.93	0.955	95.5

of the hydrophobic chain resulted in increasing $\Gamma_{\max}$ and decreasing $A_{\min}$, through enhancing the hydrophobic interactions [52]. Also, by using Eq. (8), the higher adsorption ability of surfactant (Π_{CMC}), the surface pressure at CMC, can be determined [52]:

$$\Pi_{\mathrm{CMC}} = \gamma_{0} - \gamma_{\mathrm{CMC}} \tag{8}$$

where γ_0 is the surface tension of pure solvent and γ_{CMC} is the surface tension of solution at the CMC. The Π_{CMC} value determines the extent to which the surfactant can reduce the surface tension, and evaluate the extent to which the surfactant can reduce the surface tension [52]. Π_{CMC} increased with the increase of hydrophobic chain length. Also, the thermodynamic parameters of adsorption and micellization of the synthesized cationic surfactants were calculated according to Gibb's adsorption equations as follows [53]:

$$\Delta G^{0}_{mic} = RT \ln CMC \tag{9}$$

$$\Delta G^{0}_{ads} = \Delta G^{0}_{mic} - 0.6023\pi_{CMC}A_{\min} \tag{10}$$

where c is the adsorption free energy and ΔG^{0}_{mic} is micellization free energy. The properties of the surfactants at the interface and in the bulk of their solutions depend on the thermodynamic parameters of micellization and adsorption, which were calculated and listed in Table 3. The free energies of adsorption and micellization were represented in negative values; this proves the spontaneous occurrence of such processes. Also, depending on the more negative value of the adsorption energies, these surfactants tend to be adsorbed more effectively than to be micellized.

The data in Table 3 also show that the CMC values decreases with increases in the length of the hydrocarbon chain of the investigated cationic surfactants [54]. It can be noted that the excellence of the inhibitory action of a surfactant depends on its CMC value, where the lower value gives more inhibition action. Based on this view, the surfactant 3c shows the lowest CMC value (Table 3) and, hence, it is considered the most effective corrosion inhibitor for carbon steel in 15% HCl solution. This returns to that compound 3c creates a good hydrophobic physical barrier to the aggressive ions and this account for its high inhibition efficiency.

Foaming Power and Biodegradability

Foaming is characterized for anionic and nonionic surfactants and it is one of the most important properties. Hence, these surfactants are involved into many home-care formulations. On the other hand, cationic surfactants do not form significant foam, so they are used for treatment of fabric and they possess antimicrobial activity. But, in other cases, especially during the processing, the foam must be inhibited as it may cause a very serious problem. As shown in Table 3, the synthesized cationic surfactants have low tendency toward foam formation, and thus may be used in a variety of applications such as washing machine laundry or additives in oilfield applications.

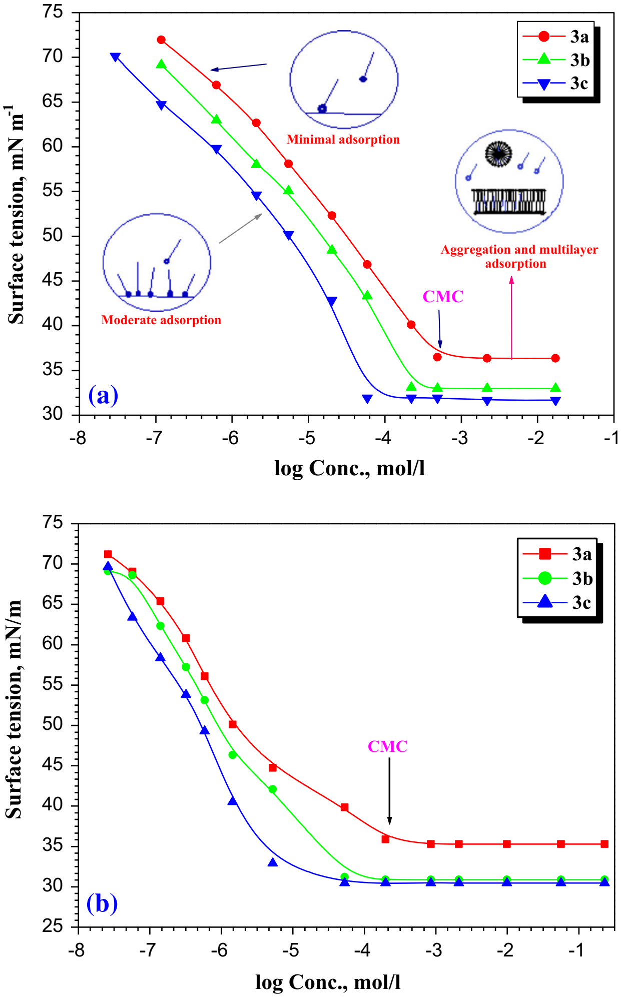

Fig. 5 Variations of the surface tension with the concentrations (C) of the synthesized cationic surfactants 3a–c in (**a**) water and (**b**) 15% HCl at 30 °C

The use of surfactants in agricultural, industrial and domestic applications leads to the entry of these compounds into terrestrial and aquatic ecosystems. It is seen from the biodegradation results in the river water via die-away tests in Table 3 that the biodegradation ratio of all of the synthesized cationic surfactants ranged from 55 to 75% after the 15th day of exposure to microorganisms. In the river water, the results of biodegradation reflected the fact that lowering of the value of surface tension is a reverse function of the biodegradation process. From the data in Table 3, it is noted that the biodegradation extent of different cationic surfactant solutions increases gradually by increasing the time and length of the hydrophobic chain. Also, it was found that the presence of a benzene nucleus in all synthesized cationic surfactants leads to decrease of the biodegradation values if compared with the other synthesized cationic surfactants [29, 45].

Table 3 Surface-active properties, foaming stability, foaming high and biodegradability of the synthesized cationic surfactants 3a–c in water and 15% HCl at 30 °C

Medium	Compounds	CMC (mM)	γ_{CMC}	Π_{CMC} (mN/m)	Γ_{max} (mol cm^{-2} × 10^{10})	Foaming stability (s)	Foaming high (ml)	Biodegradability (%) after 15 days	A_{min} (nm^2)	ΔG^o_{mic} (kJ mol^{-1})	ΔG^0_{ads} (kJ mol^{-1})
Water	3a	0.987	36.46	35.54	2.17	60	15	55	0.765	−17.361	−34.09
	3b	0.501	33.11	38.89	2.27	100	23	67	0.731	−19.122	−36.24
	3c	0.101	31.94	40.06	2.35	150	30	75	0.706	−23.148	−40.17
15% HCl	3a	0.85	35.30	36.70	1.87	–	–	–	0.880	–	–
	3b	0.20	30.87	41.13	1.95	–	–	–	0.851	–	–
	3c	0.054	30.48	41.52	2.11	–	–	–	0.782	–	–

Adsorption Isotherm and Thermodynamic Consideration

The adsorption isotherm can yield basic information about the interaction between the surfactant and the metal surface. The adsorption characteristics of the surfactants were investigated by fitting the obtained experimental results for the degrees of surface coverage (θ) into various adsorption isotherms like Temkin, Frumkin, Langmuir, Flory–Huggins, Freundlich, and Bockris–Swinkles isotherms. According to the data, it can be concluded that the best description of the adsorption behavior of 3a, 3b and 3c inhibitors can be described by the Langmuir adsorption isotherm which is expressed as follows [55]:

$$\frac{C_{inh}}{\theta} = C_{inh} + \frac{1}{K_{ads}} \tag{11}$$

where K_{ads}, C_{inh} and θ are the adsorption equilibrium constant, the inhibitor concentration and the surface coverage, respectively. Figure 6, a plot of $C_{inh.}/\theta$ vs. C_{inh} at 323 K, gives a straight line with excellent correlation coefficients ($R > 0.999$; Table 4) and slope near to unity (1.13, 1.11 and 1.09 for 3a, 3b and 3c, respectively), confirming the adsorption of all surfactants on the surface of carbon steel follows the Langmuir adsorption model. On the other hand, a slight deviation in slope values from unity is observed, suggesting interactions among the adsorbed species on the surface of the metal [56]. The obtained results indicated that the regression coefficients (R^2) values were very close to unity, which signifies strong adherence of inhibitors to the metal surface.

The values of K_{ads} calculated from the reciprocal of the intercept of isotherm lines for carbon steel at 323 K are listed in Table 4, suggesting that the synthesized inhibitors are easily and strongly adsorbed on the carbon steel surface. The values of K_{ads} are related to the free energy of adsorption (ΔG^0_{ads}) according to equation [57]:

$$K_{ads} = \frac{1}{55.5}\exp\left(-\frac{\Delta G^0_{ads}}{RT}\right), \tag{12}$$

where R is the gas constant, T is the absolute temperature and 55.5 is the molar concentration of water. The negative values of ΔG^0_{ads} (Table 4) indicate a spontaneous adsorption of the surfactant on the carbon steel surface by displacement of water molecules from the metal surface by the inhibitor and formation of a protective film [58]. Generally, the values of ΔG^0_{ads} up to -20 kJ/mol are associated with an electrostatic interaction between charged molecules and charged steel surface, physisorption, while those of -40 kJ/mol or less are associated with chemisorption as a result of sharing or transfer of electrons from the organic molecules to the metal surface to form a coordinate type of bond (chemisorption) [59]. In the present study, the values of ΔG^0_{ads} at 323 K were -33.67, -33.72 and -34.73 kJ/mol for inhibitors 3a, 3b and 3c, respectively. This indicates that the adsorption of the synthesized surfactants at the surface of carbon steel in 15% HCl solution is not pure physisorption, but it is a combination of physisorption as well as chemisorption. The adsorption of the surfactant at cathodic sites of steel reduces the hydrogen evolution [60]. In addition, the large size and high molecular weight of the surfactant molecules highly affect the inhibition efficiency of the inhibitors. Moreover, the adsorption of quaternary ammonium cations at the metal surface forms an adsorbed monomolecular layer by forming a complex on the carbon steel surface. The adsorbed layers protect the steel surfaces from Cl^- attack to prevent the iron oxidation reaction at the anode [58].

Surface Analysis by SEM and EDX After 2 days of Immersion

An SEM micrograph of carbon steel alloy before immersion is shown in Fig. 7a; it can be seen from this figure that the surface seems smooth and some abrading scratches are apparent; EDX analysis in Fig. 7b indicated that Fe is the main constituent in the alloy and the characteristic peaks are related to the metals which are present in the carbon steel alloy (Table 5). Figure 7c shows the surface appearance of the carbon steel after immersion in 15% HCl without inhibitors, displaying a heterogeneous surface with small pits of different form due to severe corrosion. In this

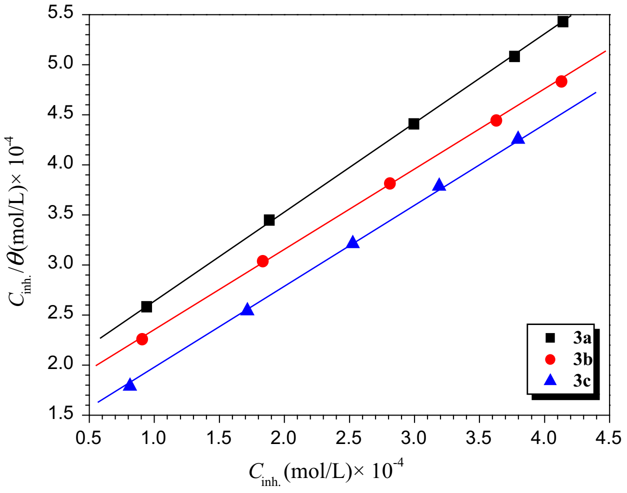

Fig. 6 Langmuir adsorption isotherm (C_i/θ vs. C_i) fitting of the obtained from Tafel polarization data for carbon steel in 15% HCl containing various concentrations of inhibitors at 50 °C

case, the EDX spectrum (Fig. 7d) described the characteristic signals of Fe, Mn, P, S, Ni and Cr, in addition to other elements, such as oxygen and Cl. This indicated that the passive film contained Fe_2O_3 and/or $FeCl_3$. The micrograph in Fig. 7e and g show the carbon steel surface in the presence of 250 ppm of 3a and 3c inhibitors, respectively. In comparison to the blank morphology (Fig. 7a), the surface in the presence of inhibitors is much less damaged and smooth. Among 3a and 3c, the presence of inhibitor 3c results into a comparatively cleaner and smoother surface. EDX analysis of carbon steel immersed in the 15% HCl containing 250 ppm of 3a and 3c compounds in Fig. 7f and h shows the additional peaks, demonstrating the existence of C and N. In addition, this figure corroborated the presence of oxygen and chloride in a lower concentration, which suggested that it decreased the kinetics of the corrosion reactions. Moreover, the carbon signal (which was very small in the blank carbon steel) was attributed to the presence of 3a and 3c molecules on the metal surface; the presence of 3a and 3c qualitatively increased the carbon content from 0.17 to 5.37 and 5.86%, respectively. Table 5 shows the percentages of the elements present on the analyzed surfaces with and without the investigated inhibitors.

Corrosion Inhibition Mechanism

The experimental data demonstrated that the corrosion inhibition effect of the investigated synthesized surfactants on steel is dependent on the adsorption of inhibitor molecules on the steel substrate. The surfactant molecule adsorption on the steel surface can be due to the existence of lone pairs of electrons, loosely bound electrons, π-electron clouds and aromaticity. Adsorption of the surfactant molecules on the steel surface can be expressed according to the following Equation [61]:

$$\mathrm{Surf}._{(\mathrm{sol.})} + x\mathrm{H_2O}_{(\mathrm{ads.})} = \mathrm{Surf}._{(\mathrm{ads.})} + x\mathrm{H_2O}_{(\mathrm{sol.})} \qquad (13)$$

where x is the number of H_2O molecules removed from the steel surface for each surfactant molecule adsorbed. Adsorption of the surfactant molecules occurs because the interaction energy between the surfactant molecules and the steel surface is greater than that between H_2O molecules and the steel surface. So, the inhibition effect by surfactants is attributed to the adsorption of the surfactant molecules through their functional groups onto the metal surface. The strength of adsorption depends on the charge on the functional groups [62]. The charge of the metal surface can be determined from the potential of zero charge (E_{PZC}) on the correlative scale (φ_c) by the equation [63]:

$$\varphi_c = E_{\mathrm{corr}} - E_{\mathrm{PZC}}. \qquad (14)$$

If the $E_{\mathrm{PZC}} > E_{\mathrm{corr}}$ of the metal in a given electrolyte, the metal surface is negatively charged, then the adsorption of cations will be most likely. For $E_{\mathrm{PZC}} < E_{\mathrm{corr}}$, the metal surface is positively charged, and the adsorption of anions is most likely. From Table 1, it was observed that the E_{corr} of carbon steel in 15% HCl solution with addition of 250 ppm of 3a, 3b and 3c compounds are −0.460, −0.455 and −0.464 V (SCE), respectively. Benerijee and Malhotra [64] reported the E_{PZC} of Fe in HCl solution is −0.530 V (SCE). Therefore, the values of φ_c re +0.070, +0.075 and +0.066 V (SCE), so the steel surface acquires a slightly positive charge. Therefore, in the present conditions, the chloride ions in the solution will first be adsorbed at the electrode/solution interface at the E_{corr} through electrostatic attraction force due to the excess positive charge at this interface. After this first adsorption of chloride ions, the electrode surface will become negatively charged. The titled inhibitor molecules exist in HCl solution as protonated through –OH, –C=O– and $–N^+$ ions and it is in equilibrium with the corresponding molecular form. Hence, the positively charged of cationic forms molecule and positively charged on $–N^+$ ion has been formed an electrostatic bond with the Cl^- ions already adsorbed on carbon steel surface. Moreover, these molecules are also adsorbed through direct interaction of the unshared lone pairs of electrons and π-electron clouds with the vacant d-orbitals of Fe to inhibit the corrosion [65].

Fig. 7 SEM micrograph (**a**) and EDX analysis (**b**) of carbon steel ▶ substrate; SEM micrograph (**c**) and EDX analysis (**d**) of carbon steel after immersed for 2 days in 15% HCl; SEM micrograph (**e**) and EDX analysis (**f**) of carbon steel after immersed for 2 days in 15% HCl with 250 ppm of 3a compound; SEM micrograph (**g**) and EDX analysis (**h**) of carbon steel after immersed for 2 days in 15% HCl with 250 ppm of 3c compound

Table 4 Thermodynamic parameters for the adsorption of the studied surfactants on carbon steel electrode in 15% HCl solution

Inhibitor code	Slope	Regression coefficients (R^2)	K_{ads} ($\mathrm{M^{-1}}$)	ΔG^o_{ads}(kJ $\mathrm{mol^{-1}}$)
3a	1.13	0.99994	6.82×10^4	−33.67
3b	1.11	0.99984	10.52×10^4	−33.72
3c	1.09	0.99992	15.38×10^4	−34.73

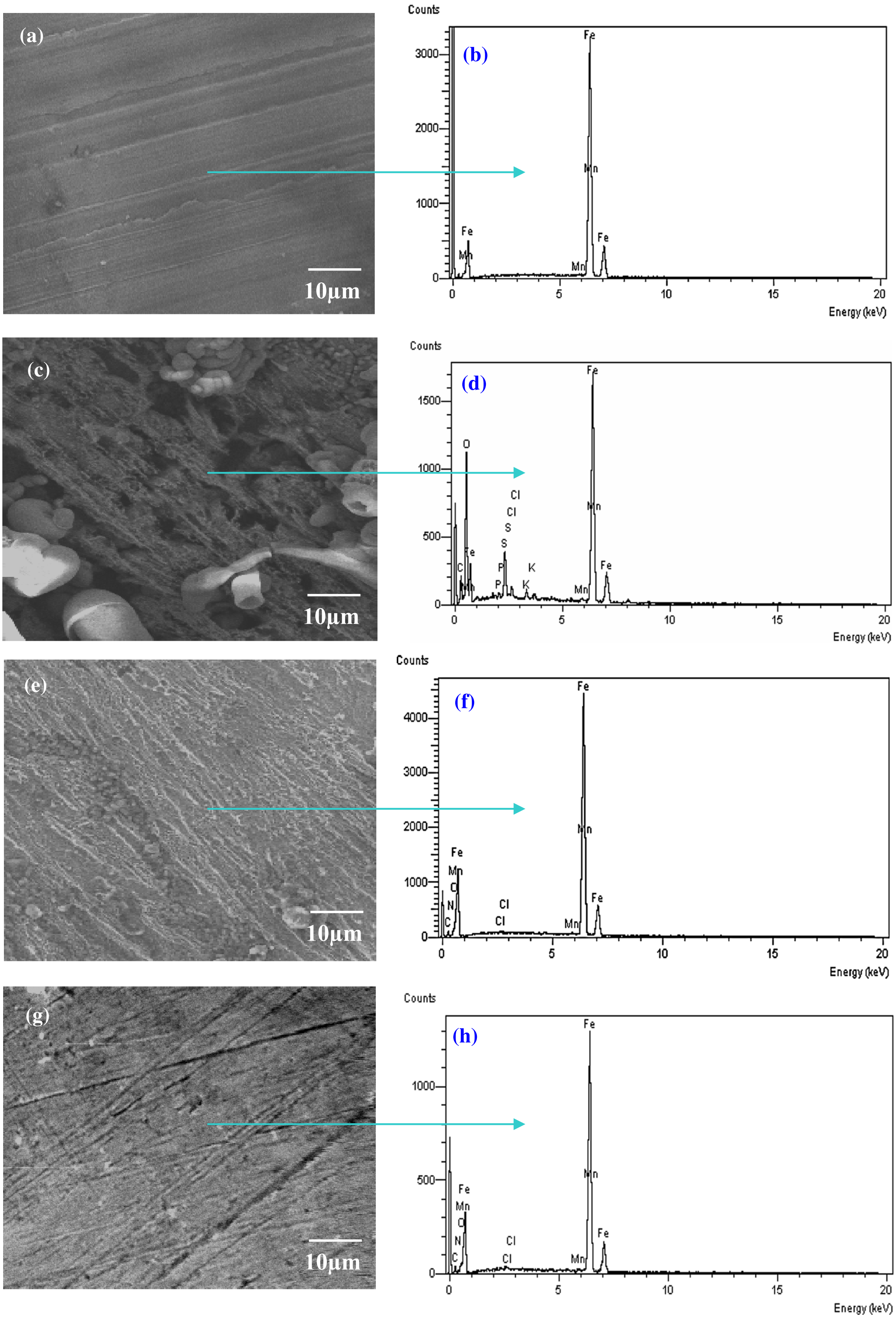
(a)
10μm
(b)
Counts
3000
2000
1000
0
Fe
Mn
Fe
Mn
Fe
Mn
0
5
10
15
20
Energy (keV)
(c)
10μm
(d)
Counts
1500
1000
500
0
Fe
O
Cl
Cl
S
S
Mn
K
P
P
K
C
Fe
Mn
Mn
Fe
0
5
10
15
20
Energy (keV)
(e)
10μm
(f)
Counts
4000
3000
2000
1000
0
Fe
Mn
Fe
Mn
O
N
C
Cl
Cl
Mn
Fe
0
5
10
15
20
Energy (keV)
(g)
10μm
(h)
Counts
1000
500
0
Fe
Mn
Fe
Mn
O
N
C
Cl
Cl
Mn
Fe
0
5
10
15
20
Energy (keV)

Table 5 Percentage atomic contents of elements obtained from EDX spectra

Test	Samples	Elements (wt.%)									
		C	Si	Ni	Mn	S	O	Cr	Fe	N	Cl
Before corrosion	Carbon steel	0.17	0.17	0.01	0.70	0.03	–	0.01	98.91	–	–
After corrosion	Carbon steel immersed in 15% HCl	0.15	0.15	0.01	0.52	0.02	32.42	–	45.42	–	21.40
	Carbon steel immersed in 15% HCl + 250 ppm 3a	5.37	0.08	–	0.43	–	12.41	–	71.54	3.41	6.76
	Carbon steel immersed in 15% HCl + 250 ppm 3c	5.86	0.01	–	0.10	–	11.71	–	73.42	3.78	5.12

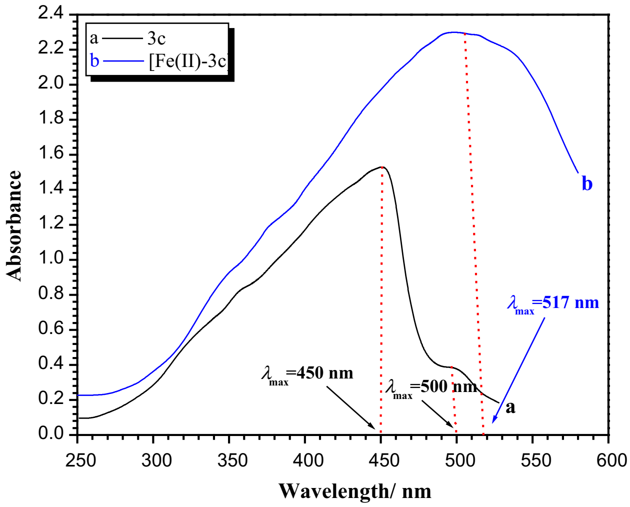

Fig. 8 UV/vis absorption of (**a**) 3c compound and (**b**) [Fe(II)–3c] complex

UV–visible absorption spectroscopy was employed to confirm the possibility of the formation of [Fe(II)–3c] complex. Figure 8 shows UV/vis absorption spectra obtained from 15%HCl solution containing 3c molecules before and after 2 days of carbon steel immersion. From UV/vis spectra obtained (Fig. 8), one can observe that the 3c compound exhibits one broad maximum at about 450 nm and small one at about 500 nm, corresponding to the $\pi \rightarrow \pi^*$ and $n \rightarrow \pi^*$ transitions, respectively. But, the [Fe(II)–3c] complex does exhibit one absorption maximum at about 517 nm. The change in band maximum suggests the interaction between the inhibitor molecule and Fe(II) ions in the solution. Abboud *et al.* [66] has stated that the change in the absorbance maximum values indicates the formation of a complex between two species in solution. The stoichiometry of the complex was determined by convenient spectrophotometric continuous variation method (c.f. Fig. S7; supporting data). The results suggested the possible formation of the 1:1 [Fe(II)–3c] complex. The complex formed directly based on donor–acceptor interactions between the π electrons and free electrons on the O atom with vacant d orbitals of Fe.

In order to support the fact that the corrosion inhibition of carbon steel in HCl solution is due to the adsorption of surfactant molecules on the surface of steel, FTIR spectra was used. The FTIR spectrum of compound 3c reveals that the peak at 3150–3400 cm^{-1} is due to an OH group, whereas at 1701 cm^{-1}, it is due to the C=O. The C–H aliphatic fatty chain is seen in the levels of 2956, 2930 and 2831 cm^{-1}. The aromatic C=C stretching frequency is observed at the level of 1600 cm^{-1}. FTIR spectrum of a film layer formed on metal surface after immersion in HCl solution containing 250 ppm 3c compounds for 2 days is shown in Fig. S8 (supporting data). The C=O stretching frequency drops from the levels of 1701 and cm^{-1} to the level of 1679 cm^{-1}. Furthermore, a new peak at 577 cm^{-1} is observed due to the Fe–O bond. This suggests that an electron cloud of C=O is shifted from C=O up to Fe^{2+}, resulting in formation of [Fe(II)–3c] complex on the metal surface [67]. The UV and FTIR results support the possibility of the complex formation between Fe^{2+} cation and surfactant molecule in 15% HCl solution.

We compared our results with the literature data. Hegazy *et al.* [30] studied the inhibition behavior of novel cationic surfactant, namely *N*,*N*′-[(oxalylbis(oxy))bis(ethane-2,1-diyl)]bis(*N*,*N*-dimethyldodecan-1-aminium bromide), for carbon steel tubes corrosion in 1.0 M HCl. They found that in the presence of 5 mM of inhibitor, the inhibition efficiency was 89.02%. Negm *et al.* [53] also investigated the inhibition performance of some new eco-friendly cationic surfactants on carbon steel in 1.0 M HCl using gravimetric and potentiodynamic techniques. They showed that the maximum inhibition efficiencies ranged between 95.09 and 98.53% at 400 ppm. Moreover, Fouda *et al.* [68] investigated the inhibition efficiencies of some cationic surfactants, namely cetyl trimethyl ammonium bromide (CTAB) and dodecyl trimethyl ammonium chloride (DTAC) in 0.5 M HCl. They found inhibition efficiencies were around 86.5 and 87.1%, respectively.

The surfactants evaluated in the present study display superior protective performance as corrosion inhibitors for the investigated working electrode in 15% HCl even at low concentrations. The inhibition efficiency of surfactant compounds follows the order: 3c > 3b > 3a. The high inhibition efficiency of these compounds is attributed to the occurrence of high electron density from the benzene ring.

The alkyl chains are arranged on the steel surface, preventing contact between the aggressive solution and the metal surface and leading to a decrease in the carbon steel dissolution [69]. By increasing the molecular length, the interaction between metal–medium increased and, hence, the efficiency of the corrosion increased. Among the investigated compounds, compound 3c displays higher *P*% values, which can be due to the long length of the hydrophobic chain ($n = 17$).

Conclusions

From the findings and discussion, the following points can be emphasized:

1. Three novel quaternary ammonium-based cationic surfactants have been synthesized, and their chemical structures were confirmed using FTIR, ^{1}H NMR and ^{13}C NMR spectroscopic methods.
2. The results of surface activities showed that increasing the hydrophobic chain length in the synthesized compounds decreases their surface tension and CMC values. The biodegradation ability of the surfactants reached the maximum (55 to 75%) within 15 days.
3. The potentiodynamic polarization and EIS results showed that the studied cationic surfactants are efficient inhibitors for carbon steel corrosion in 15% HCl solution. The inhibition efficiencies increase with the increase of inhibitor dose and reached the maximum at 250 ppm.
4. The investigated cationic surfactants have a strong ability to adsorb on the steel/solution interface. The adsorption of these surfactant inhibitors on the metal surface obeys the Langmuir isotherm, and the adsorption free energies (ΔG^0_{ads}) are around −33 kJ/mol, indicating the adsorption of inhibitor molecules on the steel surface involves both physisorption and chemisorption.
5. UV/vis and FTIR results support the possibility of complex formation between Fe^{2+} cation and surfactant molecule in 15% HCl solution.
6. The results of SEM demonstrated that the surfactant molecules formed a good protective film on the carbon steel surface.

References

1. Abd El-Lateef HM. Synergistic effect of polyethylene glycols and rare earth Ce^{4+} on the corrosion inhibition of carbon steel in sulfuric acid solution: electrochemical, computational, and surface morphology studies. Res Chem Intermed. 2016;42:3219–40.
2. Abd El-Lateef HM, Abu-Dief AM, El-Gendy BEM. Investigation of adsorption and inhibition effects of some novel anil compounds towards mild steel in H_2SO_4 solution: electrochemical and theoretical quantum studies. J Electroanal Chem. 2015;758:135–47.
3. Finšgar M, Jackson J. Application of corrosion inhibitors for steels in acidic media for the oil and gas industry: a review. Corro Sci. 2014;86:17–41.
4. Baddini ALdQ, Cardoso SP, Hollauer E, Gomes JAdCP. Statistical analysis of a corrosion inhibitor family on three steel surfaces (duplex, super-13 and carbon) in hydrochloric acid solutions. Electrochim Acta. 2007;53:434–46.
5. Quraishi M, Jamal D. Fatty acid triazoles: novel corrosion inhibitors for oil well steel (N-80) and mild steel. J Am Oil Chem Soc. 2000;77:1107–11.
6. Karthikaiselvi R, Subhashini S. Study of adsorption properties and inhibition of mild steel corrosion in hydrochloric acid media by water soluble composite poly (vinyl alcohol-omethoxy aniline). J Assoc Arab Univ Basic Appl Sci. 2014;16:74–82.
7. Growcock FB. Corrosion kinetics of J55 steel in hydrochloric acid inhibited with benzoyl allyl alcohol. Corrosion. 1989;45:393–401.
8. Frenier WW, Growcock FB, Lopp VR. a-Alkenylphenones—a new class of acid corrosion inhibitors. Corrosion. 1988;44:590–8.
9. Jasinski RJ, Frenier WW (1992) Process and composition for protecting chrome steel, in: US Patent 5,120,471, Dowell Schlumberger Incorporated, Tulsa, Okla, 7.
10. Quraishi MA, Sardar R. Dithiazolidines—a new class of heterocyclic inhibitors for prevention of mild steel corrosion in hydrochloric acid solution. Corrosion. 2002;58:103–7.
11. Williams DA, Holifield PK, Looney JR, McDougall LA (1993) Method of inhibiting corrosion in acidizing wells, in: US Patent 5,200,096, Exxon Chemicals Patents, Inc., Linden NJ.
12. Williams DA, Holifield PK, Looney JR, McDougall LA (1991) Corrosion inhibitor and method of use, in: US Patent 5,002,673, Exxon Chemical Patents Inc., Linden NJ.
13. Abd El-Lateef HM, Abbasov VM, Aliyeva LI, Ismayilov IT, Qasimov EE. Efficient complex surfactants from the type of fatty acids as corrosion inhibitors for mild steel C1018 in CO_2–environments. J Korean Chem Soc. 2013;57(1):25–34.
14. Abd El-Lateef HM, Abbasov VM, Aliyeva LI, Qasimov EE, Efremenko EN, Ismayilov TA, Mamedxanova SA, Ismayilov IT. Inhibition effects of some novel surfactants based on corn oil and diethanolamine on mild steel corrosion in chloride solutions saturated with CO_2. Int J Thin Film Sci Tec. 2013;2(2):91–105.
15. Al-Sabagh AM, Migahed MA, Awad HS. Reactivity of polyester aliphatic amine surfactants as corrosion inhibitors for carbon steel in formation water (deep well water). Corros Sci. 2006;48:813–28.
16. Nessim IM, Hamdy A, Osman MM, Shalaby MN. Inhibitory effect of some cationic gemini surfactants for carbon steel in sea water. Int J Chem. 2012;2:1–18.
17. Osman MM, El-Ghazawy RA, Al-Sabagh AM. Corrosion inhibitor of some surfactants derived from maleic-oleic acid adduct on mild steel in 1 M H_2SO_4. Mater Chem Phys. 2003;80:55–62.
18. Popova A, Christov M, Vasilev A, Zwetanova A. Mono- and dicationic benzothiazolic quaternary ammonium bromides as mild steel corrosion inhibitors. Part I: gravimetric and voltammetric results. Corros Sci. 2011;53:679–86.
19. Khamis A, Saleh MM, Awad MI. Synergistic inhibitor effect of cetylpyridinium chloride and other halides on the corrosion of mild steel in 0.5 M H_2SO_4. Corros Sci. 2013;66:343–9.
20. Soror Y, El-Ziady MA. Effect of cetyl trimethyl ammonium bromide on the corrosion of carbon steel in acids. Mater Chem Phys. 2002;77:697–703.
21. Badawi AM, Hegazy MA, El-Sawy AA, Ahmed HM, Kamel WM. Novel quaternary ammonium hydroxide cationic surfactants as corrosion inhibitors for carbon steel and as biocides for sulfate reducing bacteria (SRB). Mater Chem Phys. 2010;124:458–65.

22. Bentiss F, Traisnel M, Lagrenee M. The substituted 1,3,4-oxadiazoles: a new class of corrosion inhibitors of mild steel in acidic media. Corros Sci. 2000;42:127–46.
23. Christopher MAB, Isabel ARG, Jenny PSM. The electrochemical behavior and corrosion of aluminium in chloride media. The effect of inhibitor anions. Corros Sci. 1994;36:915–23.
24. Abbasov VM, Aliyeva LI, Abd El-Lateef HM, Ismayilov IT. some surfactants based on the vegetable oils as CO_2 corrosion inhibitors for mild steel in oilfield formation water. Int J Corros Scale Inhib. 2015;4(2):162–75.
25. Elachouri M, Hajji MS, Kertit S, Essassi EM, Salem M, Coudert R. Some surfactants in the series of 2-(alkyldimethylammonio) alkanol bromides as inhibitors of the corrosion of iron in acid chloride solution. Corros Sci. 1995;37:381–9.
26. Hamitouche H, Khelifa A, Kouache A, Moulay S. Study of the inhibiting effect of a quaternary ammonium surfactants mixture synthesized from petroleum fraction (reformate) against the carbon steel corrosion in HCl 1 M. Res Chem Intermed. 2014;40(8):2859–72.
27. Munoz A, Genesca J, Duran R, Mendoza J. Mechanism of $FeCO_3$ formation on API X70 pipeline steel in brine solutions containing CO_2. Proc NACE Corros paper No. 05297 2005.
28. Tawfik SM, Abd-Elaal AA, Shaban SM, Roshdy AA. Surface, thermodynamic and biological activities of some synthesized gemini quaternary ammonium salts based on polyethylene glycol. J Ind Eng Chem. 2015;30:112–9.
29. Abd El-Lateef HM, Tantawy AH. Synthesis and evaluation of novel series of Schiff base cationic surfactants as corrosion inhibitors for carbon steel in acidic/chloride media: experimental and theoretical investigations. RSC Adv. 2016;6:8681–700.
30. Hegazy MA, Rashwan SM, Kamel MM, ElKotb MS. Synthesis, surface properties and inhibition behavior of novel cationic gemini surfactant for corrosion of carbon steel tubes in acidic solution. J Mol Liq. 2015;211:126–34.
31. Abd El-Lateef HM, Abbasov VM, Aliyeva LI, Qasimov EE, Ismayilov IT. Inhibition of carbon steel corrosion in CO_2-saturated brine using some newly surfactants based on palm oil: experimental and theoretical investigations. Mater Chem Phys. 2013;142:502–12.
32. Abd El-Lateef HM, Abu-Dief AM, Abdel-Rahman LH, Sañudo EC, Aliaga-Alcalde N. Electrochemical and theoretical quantum approaches on the inhibition of C1018 carbon steel corrosion in acidic medium containing chloride using some newly synthesized phenolic Schiff bases compounds. J Electroanal Chem. 2015;743:120–33.
33. Abd El-Lateef HM. Experimental and computational investigation on the corrosion inhibition characteristics of mild steel by some novel synthesized imines in hydrochloric acid solutions. Corro Sci. 2015;92:104–17.
34. Abbasov VM, Abd El-Lateef HM, Aliyeva LI, Qasimov EE, Ismayilov IT, Khalaf MM. A study of the corrosion inhibition of mild steel C1018 in CO_2-saturated brine using some novel surfactants based on corn oil. Egypt J Petrol. 2013;22:451–70.
35. Liu FG, Du M, Zhang J, Qiu M. Electrochemical behavior of Q235 steel in salt water saturated with carbon dioxide based on new imidazoline derivative inhibitor. Corros Sci. 2009;51:102–9.
36. Fiori-Bimbi M, Alvarez PE, Vaca H, Gervasi CA. Corrosion inhibition of mild steel in HCl solution by pection. Corros Sci. 2015;92:192–9.
37. Saliyan VR, Adhikari AV. Quinolin -5-ylmethylene-3- {[8- (trifluoromethyl) quinolin-4-yl] thio}propanohydrazide as an effective inhibitor of mild steel corrosion in HCl solution. Corros Sci. 2008;50:55–61.
38. Noor EA, Al-Moubaraki AH. Corrosion behavior of mild steel in hydrochloric acid solutions. Int J Electrochem Sci. 2008;3:806–18.
39. Deyab MA, Abd El-Rehim SS, Keera ST. Study of the effect of association between anionic surfactant and neutral copolymer on the corrosion behavior of carbon steel in cyclohexane propionic acid. Colloids Surf A. 2009;348:170–6.
40. Hegazy MA, El-Tabei AS, Ahmed HM. synthesis of nonionic surfactants and their inhibi- tiveaction on carbon steel in hydrochloric acid. Corros Sci. 2012;64:115–25.
41. Laamari R, Benzakour J, Berrekhis F, Abouelfida A, Derja A, Villemin D. Corrosion inhibition of carbon steel in hydrochloric acid 0.5 M by hexa methylene diamine tetramethyl-phosphonic acid. Arab J Chem. 2011;4:271–7.
42. Zhang H, Wang D, Wang F, Jin X, Yang T, Cai Z, Zhang J. Corrosion inhibition of mild steel in hydrochloric acid solution by quaternary ammonium salt derivatives of corn stalk polysaccharide (QAPS). Desalination. 2015;372:57–66.
43. Chen G, Hou X, Gao Q, Zhang L, Zhang J, Zhao J. Research on Diospyros Kaki L.f leaf extracts as green and eco-friendly corrosion and oil field microorganism inhibitors. Res Chem Intermed. 2015;41:83–92.
44. Solmaz R. Investigation of adsorption and corrosion inhibition of mild steel in hydrochloric acid solution by 5-(4-Dimethylaminobenzylidene) rhodanine. Corros Sci. 2014;79:169–76.
45. Abd El-Lateef HM, Abo-Riya MA, Tantawy AH. Empirical and quantum chemical studies on the corrosion inhibition performance of some novel synthesized cationic gemini surfactants on carbon steel pipelines in acid pickling processes. Corros Sci. 2016;108:94–110.
46. Goulart CM, Esteves-Souza A, Martinez-Huitle CA, Ferreira Rodrigues CJ, Medeiros Maciel MA, Echevarria A. Experimental and theoretical evaluation of semicarbazones and thiosemicarbazones as organic corrosion inhibitors. Corros Sci. 2013;67:281–91.
47. Al-Sabagh AM, Nasser NM, Migahed MA, Kandil NG. Effect of chemical structure on the cloud point of some new non-ionic surfactants based on bisphenol in relation to their surface active properties. Egypt J Pet. 2011;20:59–66.
48. Takeshita T, Shimohara T, Maeda S. Synthesis of EDTA monoalkyl amide chelates and evaluation of the surface-active properties. J Am Oil Chem Soc. 1982;59:104–7.
49. Negm NA, El-Farargy AFM, Halim EA, El-lboudy S, Ahmed AI. Novel biobased nonionic surfactants: synthesis, surface activity and corrosion inhibition efficiency against aluminum alloy dissolution in acidic media. J Surfact Deterg. 2014;17:1203–11.
50. Badawi AM, Mohamed MAS, Mohamed MZ, Khowdairy MM. Surface and antitumor activity of some novel metal-based cationic surfactants. J Cancer Res Ther. 2007;3:198–206.
51. Alami E, Beinert G, Marie P, Zana R. Alkanediyl-alpha.,omega-bis (dimethylalkylammonium bromide) surfactants. 3. Behavior at the air–water interface. Langmuir. 1993;9(6):1465–7.
52. Rosen MJ. Surfactants and interfacial phenomena. 2nd ed. New York: Wiley; 1992.
53. Negm NA, Kandile NG, Aiad IA, Mohammad MA. New eco-friendly cationic surfactants: synthesis, characterization and applicability as corrosion inhibitors for carbon steel in 1 N HCl. Coll Surf A. 2011;391:224–33.
54. Özdil SE, Akbaş H, Boz M. Synthesis and physicochemical properties of double-chain cationic surfactants. J Chem Eng Data. 2016;61(1):142–50.
55. Da Rocha JC. Gomes JADCP, D'Elia E. Corrosion inhibition of carbon steel in hydrochloric acid solution by fruit peel aqueous extracts. Corros Sci. 2010;52(7):2341–8.
56. Mu GN, Li XH, Qu Q, Zhou J. Molybdate and tungstate as corrosion inhibitors for cold rolling steel in hydrochloric acid solution. Corros Sci. 2006;48:445–59.
57. Yıldız R, Döner A, Doğan T, Dehri İ. Experimental studies of 2-pyridinecarbonitrile as corrosion inhibitor for mild steel in hydrochloric acid solution. Corros Sci. 2014;82:125–32.

58. Al-Sabagh AM, Abd-El-Bary HM, El-Ghazawy RA, Mishrif MR, Hussein BM. Corrosion inhibition efficiency of linear alkyl benzene derivatives for carbon steel pipelines in 1 M HCl. Egypt J Petrol. 2011;20:33–45.
59. Abd El-Lateef HM, Abbasov VM, Aliyeva LI, Khalaf MM. Novel naphthenate surfactants based on petroleum acids and nitrogenous bases as corrosion inhibitors for C1018-type mild steel in CO_2-saturated brine. Egypt J Petrol. 2015;24:175–82.
60. Atta AM, El-Mahdy GA, Al-Lohedan HA, Ezzat AO. A new green ionic liquid-based corrosion inhibitor for steel in acidic environments. Molecules. 2015;20:11131–53.
61. Malik MA, HashimMA NabiF, AL-Thabaiti SA, Khan Z. Anti-corrosion ability of surfactants: a review. Int J Electrochem Sci. 2011;6:1927–48.
62. Rammelt U, Reinhard G. The influence of surface roughness on the impedance data for iron electrodes in acid solutions. Corros Sci. 1987;27:282–373.
63. Hermas AA, Morad MS, Wahdan MH. Effect of PgTPhPBr on the electrochemical and corrosion behavior of 304 stainless steel in H_2SO_4 solution. J Appl Electrochem. 2004;34:95–102.
64. Benerijee G, Malhotra SN. Contribution to adsorption of aromatic amines on mild steel surface from HCl solutions by impedance, UV, and raman spectroscopy. Corrosion (NACE). 1992;48:10–5.
65. Quraishi MA, Rawat J, Ajamal M. Dithiobiurets: a novel class of acid corrosion inhibitors for mild steel. J Appl Electrochem. 2000;30:745–51.
66. Abboud Y, Abourriche A, Saffaj T, Berrada M, Charrouf M, Bennamara A, Hannache H. A novel azo dye, 8-quinolinol-5-azoantipyrine as corrosion inhibitor for mild steel in acidic media. Desalination. 2009;237:175–89.
67. Zor S, Yazıcı B, Erbil M. Inhibition effects of LAB and LABS on iron corrosion in chlorine solutions at different temperatures. Corro Sci. 2005;47:2700–10.
68. Fouda AS, Elewady YA, Abd El-Aziz HK, Ahmed AM. Corrosion inhibition of carbon steel in 0.5 M HCl solution using cationic surfactants. Int J Electrochem Sci. 2012;7:10456–75.
69. Negm NA, Badr EA, Aiad IA, Zaki MF, Said MM. Investigation the inhibitory action of novel diquaternary Schiff dibases on the acid dissolution of carbon steel in 1 M hydrochloric acid solution. Corros Sci. 2012;65:77–86.

Dr. Hany M. Abd El-Lateef obtained his master's degree in physical chemistry from the University of Sohag, Sohag, Egypt. In 2010, he joined the Department of Chemical Resistance of Materials and Corrosion Protection, Institute of Petrochemical Processes (IPP), Azerbaijan National Academy of Sciences, as a PhD student. In 2013, he obtained his PhD from IPP in electrochemistry and corrosion science under the supervision of Professor V. M. Abbasov. His thesis dealt with the synthesis and study of corrosion inhibitors for protection from CO_2 corrosion. Since May 2013, Dr. Abd El-Lateef has been a chemistry teacher at the University of Sohag. His research has focused on unraveling corrosion mechanisms and designing corrosion-resistant alloys and coatings as well as synthesis of new inhibitors for steel pipelines, which may find application as eco-friendly corrosion inhibitors in acidizing processes in petroleum industry. Dr. Abd El-Lateef has authored 65 papers in international journals and two books.

Dr. Ahmed H. Tantawy received his bachelor's degree in chemistry from the Faculty of Science, Benha University (Benha, Egypt), in 2003. He obtained his master's degree in organic chemistry from Benha University, and then received his Ph.D. degree in petrochemical chemistry from the Institute of Petrochemical Processes (IPP), Azerbaijan National Academy of Sciences (Azerbaijan). He is a lecturer at the Chemistry Department, Faculty of Science, Benha University, Egypt. His main interest is synthesis and application of surfactants.

Dr. Antar A. Abdelhamid received his bachelor's degree in chemistry from South Valley University (Sohag, Egypt), in 2002. He then received his Ph.D. degree in organic chemistry from Baku University (Azerbaijan). He is currently a Lecturer of Chemistry at the Department of Chemistry, Faculty of Science, Sohag University, Egypt. As a researcher, he is currently interested in synthesis of organic compounds and their applications.